Dominant-Negative Histone H3 Lysine 27 Mutant Derepresses Silenced Tumor Suppressor Genes and Reverses the Drug-Resistant Phenotype in Cancer Cells

Phillip H. Abbosh,[1] John S. Montgomery,[1] Jason A. Starkey,[2] Milos Novotny,[2] Eleanor G. Zuhowski,[3] Merrill J. Egorin,[3] Annie P. Moseman,[1] Adam Golas,[1] Kate M. Brannon,[1] Curtis Balch,[1] Tim H.M. Huang,[4] and Kenneth P. Nephew[1]

[1]Medical Sciences, School of Medicine; [2]Department of Chemistry, Indiana University, Bloomington, Indiana; [3]Department of Medicine, Division of Hematology-Oncology, University of Pittsburgh Cancer Institute, Pittsburgh, Pennsylvania; and [4]Human Cancer Genetics Program, Department of Molecular Virology, Immunology, and Medical Genetics, Comprehensive Cancer Center, The Ohio State University, Columbus, Ohio

Abstract

Histone modifications and DNA methylation are epigenetic phenomena that play a critical role in many neoplastic processes, including silencing of tumor suppressor genes. One such histone modification, particularly at H3 and H4, is methylation at specific lysine (K) residues. Whereas histone methylation of H3-K9 has been linked to DNA methylation and aberrant gene silencing in cancer cells, no such studies of H3-K27 have been reported. Here, we generated a stable cell line overexpressing a dominant-negative point mutant, H3-K27R, to examine the role of that specific lysine in ovarian cancer. Expression of this construct resulted in loss of methylation at H3-K27, global reduction of DNA methylation, and increased expression of tumor suppressor genes. One of the affected genes, *RASSF1*, was shown to be a direct target of H3-K27 methylation–mediated silencing. By increasing DNA-platinum adduct formation, indicating increased access of the drug to target DNA sequences, removal of H3-K27 methylation resensitized drug-resistant ovarian cancer cells to the chemotherapeutic agent cisplatin. This increased platinum-DNA access was likely due to relaxation of condensed chromatin. Our results show that overexpression of mutant H3-K27 in mammalian cells represents a novel tool for studying epigenetic mechanisms and the Histone Code Hypothesis in human cancer. Such findings show the significance of H3-K27 methylation as a promising target for epigenetic-based cancer therapies. (Cancer Res 2006; 66(11): 5582-91)

Introduction

Chromatin structure affects numerous diverse aspects of cell biology, ranging from genomic integrity and telomere maintenance to gene activation and silencing. Chromatin architecture can be influenced by a number of covalent alterations to protein and DNA, including histone modifications and DNA methylation. One histone modification, methylation of lysine, has recently been a subject of intense study, particularly as it relates to the transcriptional status of genes and chromatin structure. A repressive histone modification, methylation of H3-K27, is mediated by proteins in the *Polycomb* group (PcG) family of genes, originally identified as genes suppressing the development of extra sex combs in *Drosophila melanogaster* (1). PcG repressors form multiple, unique complexes to suppress gene expression (2–4). Specifically, PcG complexes containing the histone methyltransferase E(z) (in *Drosophila*) or EZH2 (in humans) silence chromatin via methylation of H3-K27 (2, 5–7). EZH2 was recently shown to be overexpressed in advanced prostate (8) and breast (9) cancers. In normal fibroblasts, forced overexpression of EZH2 can induce transformation and increase invasiveness whereas EZH2 knockdown in cancer cells results in decreased proliferation (8, 9). Moreover, another PcG gene, *SU(Z)12*, has been shown to be up-regulated in a number of human tumors and exists in a repressive complexes with EZH2 (10), further implicating PcG proteins and consequently H3-K27 methylation in the development of tumor phenotypes.

Despite findings of altered methyltransferase activity in cancer, more direct studies of histone modifications are needed to categorically determine their precise role in tumorigenesis and other cellular events. The Histone Code Hypothesis is now widely accepted, due in large part to yeast genetic studies in which components of chromatin or chromatin-modifying enzymes have been manipulated (11, 12). However, because mammalian cells contain multiple copies of each histone and multiple (often redundant) chromatin-modifying enzymes, similar genetic approaches have proved much more difficult. Consequently, mammalian studies of histone methylation have been limited primarily to specific methyltransferase gene knockouts in mice (13, 14), which are technically difficult and time-consuming. Furthermore, even fewer studies have specifically addressed the status, causes, and consequences of histone methylation in cancer.

In the present study, we sought to directly examine the role of H3-K27 methylation in cancer cells. By overexpressing a dominant-negative histone transgene incapable of being methylated (due to an arginine-for-lysine mutation, H3-K27R), we successfully reduced global levels of H3-meK27 in human ovarian cancer CP70 cells, a cell line highly resistant to the chemotherapeutic agent cisplatin (15). Removal of H3-meK27 in CP70 cells resulted in altered chromatin structure and composition, reexpression of tumor suppressor genes, and resensitization to cisplatin. Further, we show concordance between DNA methylation and H3-K27 methylation. Our data indicate that the mechanism of chemosensitization may be due to "loosened" chromatin, allowing increased interactions between DNA-damaging agents and DNA, in addition to changes in gene expression. Our results may provide

Note: Supplementary data for this article are available at Cancer Research Online (http://cancerres.aacrjournals.org/).

Requests for reprints: Kenneth P. Nephew, Medical Sciences, School of Medicine, Indiana University, 302 Jordan Hall, 1001 East 3rd Street, Bloomington, IN 47405-4401. Phone: 812-855-9445; Fax: 812-855-4436; E-mail: knephew@indiana.edu.

doi:10.1158/0008-5472.CAN-05-3575

novel insight into the mechanism(s) of DNA damage acquired by tumor cells after treatment with platinum-based therapies.

Materials and Methods

Materials. CP70 cells were kindly provided by Robert Brown (Beatson Cancer Center, University of Glasgow, Glasgow, United Kingdom). Anti-2x-H3-$(me)_3$-K27 was kindly provided by Dr. Thomas Jenuwein (University of Vienna, Vienna, Austria). Anti-MBD2 antibody was kindly provided by Dr. Paul Wade (National Institute of Environmental Health Sciences, Research Triangle Park, NC). Mouse anti-H3-$(me)_3$-K9, mouse anti-H3-$(me)_3$-K27, and rabbit anti–COOH-terminal H3 antibodies were purchased from Abcam (Cambridge, MA). pIRES2-H3-EGFP and pIRES2-H3-K27R-EGFP were created by Keyclone Labs (Cincinnati, OH). pIRES2-EGFP (Clontech, Mountain View, CA) contains a multiple cloning site between the cytomegalovirus promoter and an internal ribosomal entry site. The plasmid encodes a bicistronic mRNA in which the second cistron is enhanced green fluorescent protein (EGFP). Cisplatin (Sigma-Aldrich, St. Louis, MO) was dissolved in 0.9% NaCl and used at the indicated doses. LY294002 was purchased from Sigma-Aldrich. Pooled siGENOME small interfering (siRNA) for EZH2, siCONTROL, and DharmaFECT reagent 1 were purchased from Dharmacon (Chicago, IL).

Creation and isolation of stable cell lines. Point mutations of the H3 sequence were created with arginine substituted for lysine at the amino acid position 27 under the assumption that the initial methionine was not translated (16). One day after transfection, cells were sorted using a FACScalibur instrument (BD Biosciences, San Jose, CA) for EGFP fluorescence. Transformants were selected in G418 (750 μg/mL) for at least 2 weeks and then maintained in 500 μg/mL G418 for the remainder of the study. All transgene-expressing cells used in this study were from passage 20 or earlier.

Transfection of siRNA for EZH2. Cells were plated 24 hours before transfection in 10-cm dishes. Transfection was scaled up according to the instructions of the manufacturer. Cells were grown in serum-free transfection medium for 48 hours followed by a 36-hour recovery period in complete medium. Negative controls consisted of a mock transfection containing DharmaFECT reagent 1 but no siRNA and a transfection with siCONTROL. Cells were then harvested for RNA, DNA, and protein analyses as described below.

Western blot analysis. Twenty micrograms of protein were separated by SDS-PAGE on gels containing 15% polyacrylamide. Proteins were transferred to polyvinylidene difluoride membranes and blotted with rabbit anti-2x-H3-$(me)_3$-K27 (1:4,000) or mouse anti–glyceraldehyde-3-phosphate dehydrogenase (1:500; Chemicon, Temecula, CA). Horseradish peroxidase–conjugated secondary antibodies (1:10,000; KPL, Gaithersburg, MD) or IR-dye conjugated secondary antibodies (1:10,000 anti-rabbit or 1:5,000 anti-mouse; LI-COR Biosciences, Lincoln, NE) were used for detection. Protein bands were then quantitated using ChemiDoc imaging system (Bio-Rad Laboratories, Hercules, CA) or the Odyssey Imaging System (LI-COR Biosciences).

Immunofluorescence. Cells were plated on coverslips and fixed the following day in 4% paraformaldehyde. Cells were permeabilized, blocked, and incubated with 1:4,000 anti-2x-H3-$(me)_3$-K27, counterstained with 10 μg/mL Hoechst 33258, and mounted. Images were captured on a Nikon E800 Epifluorescent inverted microscope using Metamorph 6.1 software (Molecular Devices, Sunnyvale, CA).

Chromatin immunoprecipitation. Approximately 5×10^7 cells were incubated in 1% formaldehyde at 37°C and then lysed in lysis buffer [1% SDS, 5 mmol/L EDTA, 50 mmol/L Tris-HCl (pH 8.1), antiproteases; Calbiochem, San Diego, CA]. Sonicated chromatin (200-1,000 bp in length) was immunoprecipitated from 4 mL of diluted lysate [A_{260} = 0.8; 1% Triton X-100, 2 mmol/L EDTA, 20 mmol/L Tris (pH 8.1), 150 mmol/L NaCl]. Anti-2x-H3-$(me3)_3$-K27 and anti-MBD2 were used at 1:4,000 and 1:500 dilutions, respectively. Beads were washed and eluted in 1% SDS/0.1 mmol/L $NaHCO_3$. DNA was extracted with phenol/chloroform, precipitated with ethanol, and resuspended in 20 μL of double-distilled water; 2 μL were used per 25-μL PCR reaction. Samples were analyzed in duplicate for the presence of target loci by PCR amplification for 32 cycles. Primer sequences are available on request.

Reverse transcription-quantitative PCR. RNA (2 μg) from each cell line (n = 3) was reverse transcribed using Moloney murine leukemia virus reverse transcriptase (Promega, Madison, WI) according to the instructions of the manufacturer and then diluted to 10 ng/μL. Amplification was done for 40 cycles using LightCycler FastStart DNA Master^{PLUS} SYBR Green I (Roche Applied Science, Indianapolis, IN) according to the instructions of the manufacturer using 40 ng equivalent of cDNA as template. One reaction was done for each reverse transcriptase sample. Analysis was done using the ΔÄ method; second-derivative maximum values were used for internal control gene (*ACTB, EEF1A1*, or *GUSB*) or target genes. Values are expressed as relative value ± SD; P values were calculated using two-tailed t tests. Primer sequences are available on request.

Capillary electrophoresis. Genomic 5-methyl-cytosine (5-meC) levels were determined by capillary electrophoresis as previously described (17) with slight modification. The derivatized sample was diluted 1:40 in running buffer [75 mmol/L SDS/17 mmol/L sodium phosphate/15% methanol (pH 9.0)] and separated on the MDQ capillary electrophoresis system (Beckman Coulter, Fullerton, CA) at 17 kV, 25°C. The 5-meC peak area was normalized to cytosine peak area. Three independent derivatizations were analyzed in triplicate for each cell line; statistical differences were determined using ANOVA.

Atomic absorption spectroscopy. Platinum concentration was assessed by with a Model 1100 flameless atomic absorption spectrophotometer (Perkin-Elmer, Boston, MA), monitoring at 265.9 nm. The temperature program used was as follows: ramp over 30 seconds to 90°C and hold for 30 seconds; ramp over 10 seconds to 110°C and hold for 10 seconds; ramp over 30 seconds to 300°C and hold for 30 seconds; ramp over 45 seconds to 1,500°C and hold for 60 seconds; and atomize at 2,700°C without ramping. Argon gas flow was 800 mL/min for all heating steps except during atomization (when it was interrupted). Platinum concentrations were determined by comparison with a standard curve done on the same day as the assay.

Bisulfite sequencing. DNA was bisulfite converted and bisulfite sequencing and combined bisulfite restriction analysis (COBRA) primers, designed specifically to exclude CpG dinucleotides, were used in PCR for 35 cycles. For bisulfite sequencing, a cleanup step was used to purify the product (QiaPrep Spin kit, Qiagen, Valencia, CA). The TOPO TA kit was used to clone purified products (Invitrogen, Carlsbad, CA). Sequencing from plasmid pCR2.1 was done using the M13 forward primer with Applied Biosystems Big Dye Sequencing mix (Foster City, CA) according to the instructions of the manufacturer. Ten clones of each product were aligned and the percentage of CpG methylation was calculated for each site. For COBRA, the product was digested by the enzyme indicated (all enzymes from NEB, Ipswich, MA).

Micrococal nuclease assay. Nuclei (10^6) were digested in prewarmed digest buffer (15 mmol/L Tris-HCl, 100 mmol/L KCl, 1 mmol/L $CaCl_2$, 3 mmol/L $MgCl_2$, 20% glycerol, and 15 mmol/L β-mercaptoethanol) with 600, 150, 37.5, or 9.4 mU of micrococcal nuclease (Sigma-Aldrich) for 10 minutes at 37°C. Two hundred microliters of stop solution [50 mmol/L Tris (pH 7.5), 150 mmol/L NaCl, 50 mmol/L EDTA, 10 μg/mL proteinase K] were added, followed by DNA isolation and separation on 1.6% agarose. Digested DNA (80 ng) was used for each 25-μL PCR reaction.

Assessment of cell proliferation. One day before drug treatment, cells were seeded in 96-well dishes (2,000 per well). The following day, cells were treated with cisplatin for 3 hours, followed by a 3-day recovery period. Alternatively, cells were treated with paclitaxel for 15 hours, followed by a 2-day recovery period. Following drug treatments, cells were incubated in a final concentration of 0.4 mg 3-(4,5-dimethylthiazol-2-yl)-2,5-diphenyltetrazolium bromide (MTT)/mL for 4 hours, then dissolved in 150 μL of DMSO and agitated for 10 minutes. Absorbance of each well was then read at 600 nm using a Bio-Tek (Winooski, VT) ELX-800 microplate absorbance reader. To determine the percentage of surviving cells, the average absorbance for each dose was normalized to the average absorbance for untreated cells. MTT assays were also done to determine growth rate, except that the average absorbance for each day was compared with the average absorbance on day 1. Values displayed are the average of 8 or 16 wells (mean ± SD).

Doxorubicin fluorescence microscopy. Cells were plated on poly-L-lysine–coated slides overnight. The next day, cells were treated with 10 nmol/L doxorubicin (Sigma-Aldrich) for 4 hours, then fixed at 37°C for 20 minutes in buffered 4% paraformaldehyde. Cells were made permeable with TBS-Tx [150 mmol/L NaCl, 10 mmol/L Tris-HCl (pH 7.4), 1% Triton X-100] and stained with 10 μg/mL 4′,6-diamidino-2-phenylindole (DAPI) in TBS-Tx for 5 minutes. Negative control slides consisted of DAPI only or doxorubicin only. Imaging was done using the SoftWorx program on a DeltaVision deconvoluting microscope. Optical sections were taken at 0.2-μm intervals through entire nuclei. Deconvolved images were and analyzed using MetaMorph version 6.1. A "DAPI-on-DAPI" image was created to set the color threshold for overlaid images. Then, doxorubicin and DAPI images were overlaid and measured for overlapping signals using the DAPI-on-DAPI threshold settings. The percentage of overlapping signal was calculated by dividing the thresholded area by the total nuclear area of either DAPI or doxorubicin.

Results

Isolation and characterization of stable cell lines containing point mutations in H3. CP70 cells stably expressing H3-K27R protein were generated using the plasmid pIRESII-H3-K27R-EGFP, encoding a bicistronic mRNA bisected by an internal ribosomal entry site. In this plasmid, the first cistron is H3-K27R and the second is EGFP. Cells expressing high levels of EGFP (and thus also the K27R transgene) were isolated by FACS and pooled (referred to as K27R cells). Untransfected CP70 cells and CP70 cells transfected with pIRESII-EGFP (referred to as EGFP cells) or pIRESII-H3-EGFP (referred to as wtH3 cells) were used as controls. To verify inhibition of lysine methylation, H3-$(me)_3$-K27 levels in K27R cells were analyzed by Western blot. A marked decrease ($\sim$75%) of H3-$(me)_3$-K27 was seen when K27R and CP70 cells were compared (Fig. 1*A*), which was further confirmed by immunocytochemical analyses (Fig. 1*B*). No change in either H3-$(me)_3$-K9 or H4-$(me)_3$-K20 was observed in K27R cells (Supplementary Fig. S1). Negligible H3-$(me)_3$-K27 staining was seen in normal ovarian surface epithelial cells (data not shown). No morphologic differences between CP70, wtH3, EGFP, and K27R cells were observed.

To examine the relationship between K27 methylation and PcG-mediated effects, CP70 cells were treated with LY294002 to up-regulate EZH2 methyltransferase activity (18). No effect on H3-$(me)_3$-K27 was observed (Supplementary Fig. S2), perhaps due to differences between acute/transient changes in H3-K27 methyltransferase activity (Supplementary Fig. S2 and S4, described below) versus stable dominant-negative suppression (Fig. 1).

Global CpG methylation is decreased in K27R cells. As H3-K9 methylation was previously shown as linked to DNA methylation (19–21), we explored a similar relationship with H3-K27. To determine overall DNA methylation, capillary electrophoresis was used to ascertain global 5-meC levels (described in Materials and Methods). In CP70, wtH3, EZH2 siRNA–treated CP70, and K27R cells, 5-meC levels were 4.8%, 3.5%, 3.5%, and 1.8%, respectively, of total cytosine (Fig. 1*C* and *D*), representing a significant total reduction of 5-meC in the lysine-mutated line (63% decrease K27R versus CP70, $P < 0.001$; 49% decrease K27R versus wtH3, $P < 0.001$; 27% decrease EZH2 knockdown versus CP70, $P < 0.001$). These results indicate that hypomethylation of H3-K27 leads to decreased CpG methylation. The magnitude of the decrease in DNA methylation we observed in K27R cells was comparable to that seen in cancer cells treated with the DNA methylation inhibitor 2′-deoxy-5-azacytidine for 3 days (22). In addition, we examined the reciprocal effect, DNA hypomethylation on H3-K27 methylation, using Western blot analysis. Treatment of CP70 cells with 5 μmol/L 2′-deoxy-5-azacytidine (a DNA methyltransferase inhibitor) for 72 hours resulted in a 26% decrease in H3-$(me)_3$-K27 ($P = 0.05$, Fig. 1*C*). The latter result shows that the relationship between H3-K27 and DNA methylation is bidirectional (i.e., variation in each of these epigenetic modifications can also alter the other).

Derepression of tumor suppressor gene expression in K27R cells. Because methylation of H3-K27 is widely associated with PcG-mediated gene silencing (2, 3, 6, 7), we examined expression of tumor suppressor genes frequently silenced in ovarian cancer (23–25), genes associated with cisplatin resistance (26), and genes identified as targets of PcG silencing (6). Up-regulation of 3- to 16-fold of hMLH1, ARHI, and RASSF1A tumor suppressor gene expression was observed in K27R cells as compared with the parental CP70, EGFP, and/or wtH3 cells (Fig. 2*A-C*). We then determined the expression of genes known to be down-regulated during acquisition of cisplatin resistance (26), anticipating that such genes might be up-regulated in K27R cells. Accordingly, CYT19 was up-regulated 15-fold in K27R cells compared with the parental CP70 cells ($P < 0.001$; Fig. 2*D*). Lastly, K27R cells were analyzed for expression of genes previously deemed as bona fide PcG targets in SW480 colon cancer cells (6), including *RDC1, EML4, PSMD11, CNTFR, NKX2.3, SLC25A3, KIS, TRIM52*, and *WNT1*. Within this group, only *NKX2.3* gene expression was altered from control cell lines and its expression was unexpectedly down-regulated (Fig. 2*E*), perhaps because targets of PcG-mediated silencing have been shown to be cell specific (3, 4).

To further investigate and clarify the connection between H3-K27 mutation and PcG function, we took a functional knockdown (siRNA) and pharmacologic approach to deplete EZH2 levels or activate its methyltransferase activity in CP70 cells and examine the subsequent effect on tumor suppressor gene expression. As shown in Supplementary Fig. S4, EZH2 mRNA levels were reduced by 60% ($P < 0.001$) following siRNA treatment; however, levels of EED (another PcG gene) were not altered, showing specificity of the EZH2 siRNAs. Additionally, no change in RASSF1A or ARHI expression was observed by reverse transcription-quantitative PCR. Furthermore, treatment of CP70 cells with LY294002 did not alter the expression of RASSF1A, ARHI, or NKX2.3 (Supplementary Fig. S5). These results highlight the effects of an acute/transient change in PcG-mediated silencing using siRNA versus a stable mutation introduced into K27R cells.

***RASSF1* is a direct target of H3-K27-mediated silencing in CP70 cells.** As H3-K27 methylation is a transcription-suppressive histone mark in chromatin (2, 5–7), loss of H3-meK27 in CP70 cells would be expected to derepress genes (including tumor suppressors) silenced via this modification. Therefore, we determined whether the tumor suppressor *RASSF1* is directly regulated by H3-K27 or DNA methylation. To this end, we did chromatin immunoprecipitation assays using antibodies specific for H3-$(me)_3$-K27 and methyl CpG-binding protein-2 (MBD2) to coimmunoprecipitate DNA, followed by PCR using primers spanning the *RASSF1* promoter and CpG island (Supplementary Fig. S6). As shown in Fig. 3*A*, the *RASSF1* promoter was bound by MBD2 protein and histones bearing low amounts of H3-$(me)_3$-K27 in CP70 cells. Accordingly, in K27R cells, neither H3-$(me)_3$-K27 nor MBD2 protein was detected at this promoter, suggesting that the *RASSF1* promoter/CpG island and first exon are regulated by methylation of H3-K27 in CP70 cells.

To investigate the role of DNA methylation in *RASSF1* regulation, we bisulfite sequenced two CpG islands found in the upstream regions of *RASSF1*. One CpG island contains the promoter and first

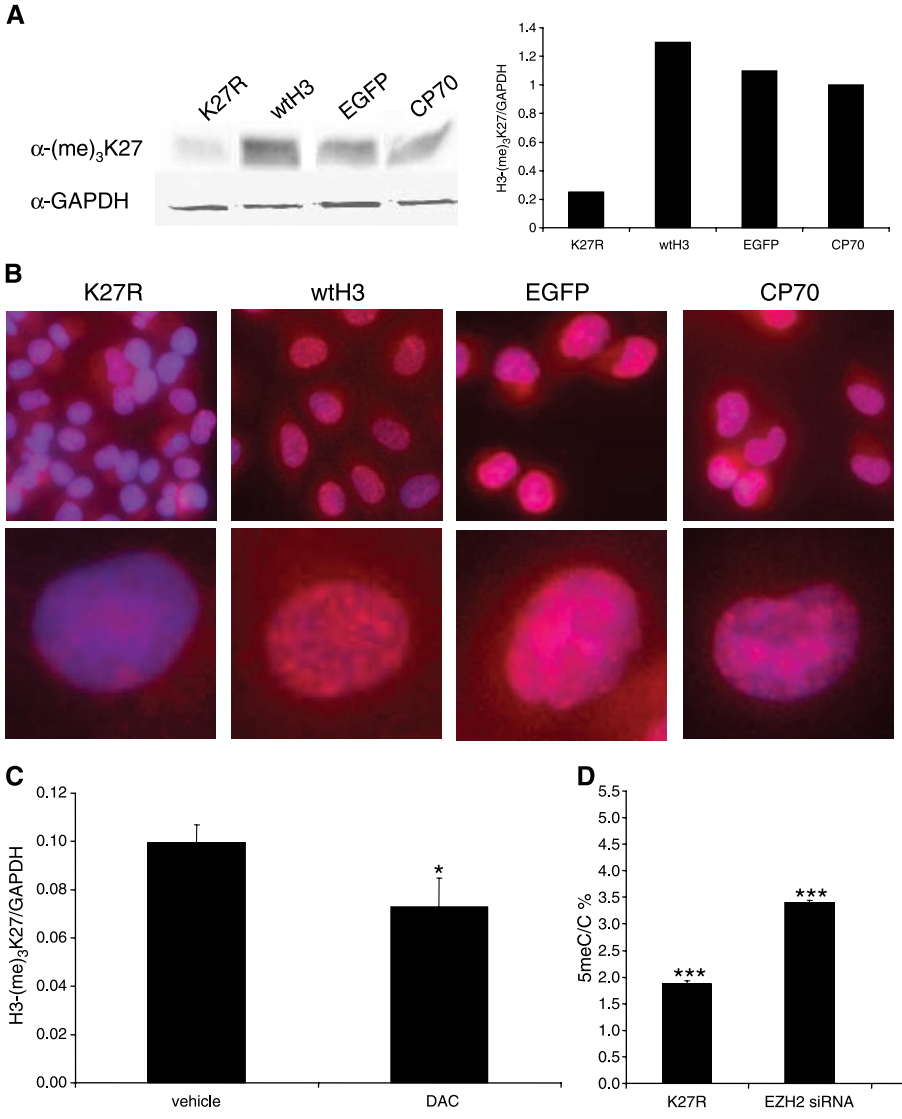

Figure 1. H3-$(me)_3$-K27 is dramatically reduced in K27R cells. *A, right,* representative Western blot analysis of K27 methylation levels in the cell lines; *left,* quantitation of Western blot. *B,* micrographs of transgene-expressing cells and control cells, confirming the loss of H3-$(me)_3$-K27. Hoechst stain is blue and H3-$(me)_3$-K27 is red. *C,* quantification of Western blot showing that H3-$(me)_3$-K27 is 26% decreased after 72-hour 2′-deoxy-5-azacytidine treatment. *Columns,* average of four quantitated bands; *bars,* SD. $P = 0.05$ (*t* test). *D,* 5-meC content is decreased in K27R and EZH2 knockdown cells compared with CP70 cells. *Columns,* average of three samples measured in triplicate; *bars,* SD. ***, $P < 0.001$ (ANOVA).

exon (1,000 bp), the other is contained within the first intron (1,700 bp). The upstream *RASSF1* CpG island was completely methylated in both cell lines whereas the intronic CpG island was completely unmethylated in both cell lines (Fig. 3*B*). Furthermore, similar results were obtained using COBRA to analyze CpG sites outside of the bisulfite sequenced regions (Fig. 3*C*).

Because loss of promoter MBD2 occupancy in K27R cells provides only indirect evidence for DNA hypomethylation, we used a micrococcal nuclease assay to determine whether the *RASSF1* promoter/CpG island resided within heterochromatin or euchromatin. Chromatin digested with micrococcal nuclease from K27R or CP70 cells seemed to be generally similar when separated electrophoretically (Fig. 3*C*). We hypothesized that if a gene (i.e., *RASSF1*) resided within heterochromatin, large fragments of the promoter/CpG island could be amplified from chromatin fragments created by restriction with micrococcal nuclease because *RASSF1* would remain in compacted chromatin and thus resistant to digestion. By contrast, if the gene resided within euchromatin, loss of the PCR product would be observed due to increased nuclease digestion. We recombined the forward and reverse primers from several products used in the chromatin immunoprecipitation assay to amplify long regions of the promoter/CpG island for 28 cycles of PCR. Using this approach, we observed loss of the *RASSF1* PCR product in micrococcal nuclease–digested K27R cells, but not in CP70 cells, except when the reaction contained low amounts of micrococcal nuclease (Fig. 3*D, top*). Additionally, two heterochromatin repeat elements that become partially hypomethylated in cancers (27), *NBL2* and *D4Z4*, remained intact after micrococcal nuclease digestion whereas the promoter of a highly expressed housekeeping gene, *EEF1A1*, remained digestion sensitive (Fig. 3*D, middle* and *bottom*). These control digestions/amplifications indicate that micrococcal nuclease-PCR is specific for dense regions of chromatin. Taken together, these results indicate that the *RASSF1* promoter, although not detectably hypomethylated, resides within decondensed and transcriptionally active DNA in K27R cells.

Loss of H3-K27 methylation resensitizes ovarian cancer cells to cisplatin. Previously, we and others have shown that DNA

methylation inhibitors can resensitize drug-resistant cells to cisplatin (28, 29), suggesting that drug-response genes may be silenced by chromatin condensation. As H3-meK27, like 5-meC, is a repressive chromatin mark and its removal induced the expression of several tumor suppressors (Fig. 2), we used MTT assays to compare cisplatin sensitivities in K27R and control cells. Significant growth inhibition following cisplatin treatment was observed for K27R cells, compared with the control cell lines, resulting in a 4-fold reduction in the cisplatin IC_{50} (10 versus 40 μmol/L in K27R cells versus control cell lines, respectively; Fig. 4*A*). No difference in the response of the K27R cells versus control cell lines to paclitaxel (IC_{50} of 7.5 and 5 nmol/L for K27R and CP70, respectively; Fig. 4*B*) or doxorubicin (IC_{50} of 60 nmol/L for both CP70 and K27R cells; data not shown) was observed, indicating a specific sensitization to cisplatin. We also found that the cisplatin IC_{50} was not altered by EZH2 knockdown when compared with mock-transfected and siCONTROL-transfected cells (Supplementary Fig. S7). We did, however, find that K27R cells grew more slowly than control cell lines (Fig. 4*C*). Growth inhibition was similar to inhibition previously seen with 2′-deoxy-5-azacytidine, resulting in a comparable (~60%) reduction of DNA methylation (28). Collectively, these experiments show that global alterations to chromatin structure result in changes in sensitivity to specific chemotherapies.

Relationship between chromatin and chemosensitivity. Cisplatin sensitization in K27R cells seemed to be mediated, in part, by changes in gene expression. However, H3-K27 hypomethylation and/or DNA hypomethylation could also alter chromatin structure, which in turn could affect platinum adduct formation by reducing steric hindrance of DNA target sequences, thus increasing drug accessibility. Because H3-K27 methylation is a mark of heterochromatin (30), chromatin compaction may be lost in K27R cells, allowing increased DNA damage at lower cisplatin doses. To investigate this possibility, CP70 and K27R cells were treated with increasing doses of cisplatin for 3 hours and immediately harvested for quantification of platinum adducts using atomic absorption spectroscopy as previously described (31). With increasing drug doses, the acquisition rate of platinum adducts in K27R cells was 2- to 4-fold greater than the rate in CP70 (Fig. 5*A*), suggesting that K27R cells possess a more open chromatin configuration, allowing for greater formation of platinum adducts.

Because DNA repair is an induced process that follows adduct formation (32), it is unlikely that the observed increase in platinum adduction was due to decreased repair (no recovery/repair period was allowed in the assay). Moreover, continuous incubation with cisplatin, even during repair, should result in continued adduct formation. However, the observed decrease in cell growth could be due to decreased DNA repair. As altered nucleotide excision repair has been shown to play a role in cisplatin resistance (32), we investigated DNA repair and the nucleotide excision repair pathway in K27R and CP70 cells by quantitating basal levels of ERCC1, a key protein in nucleotide excision repair–mediated repair (33), in each cell line. No difference in *ERCC1* expression between K27R and CP70 cells was observed, although slightly reduced

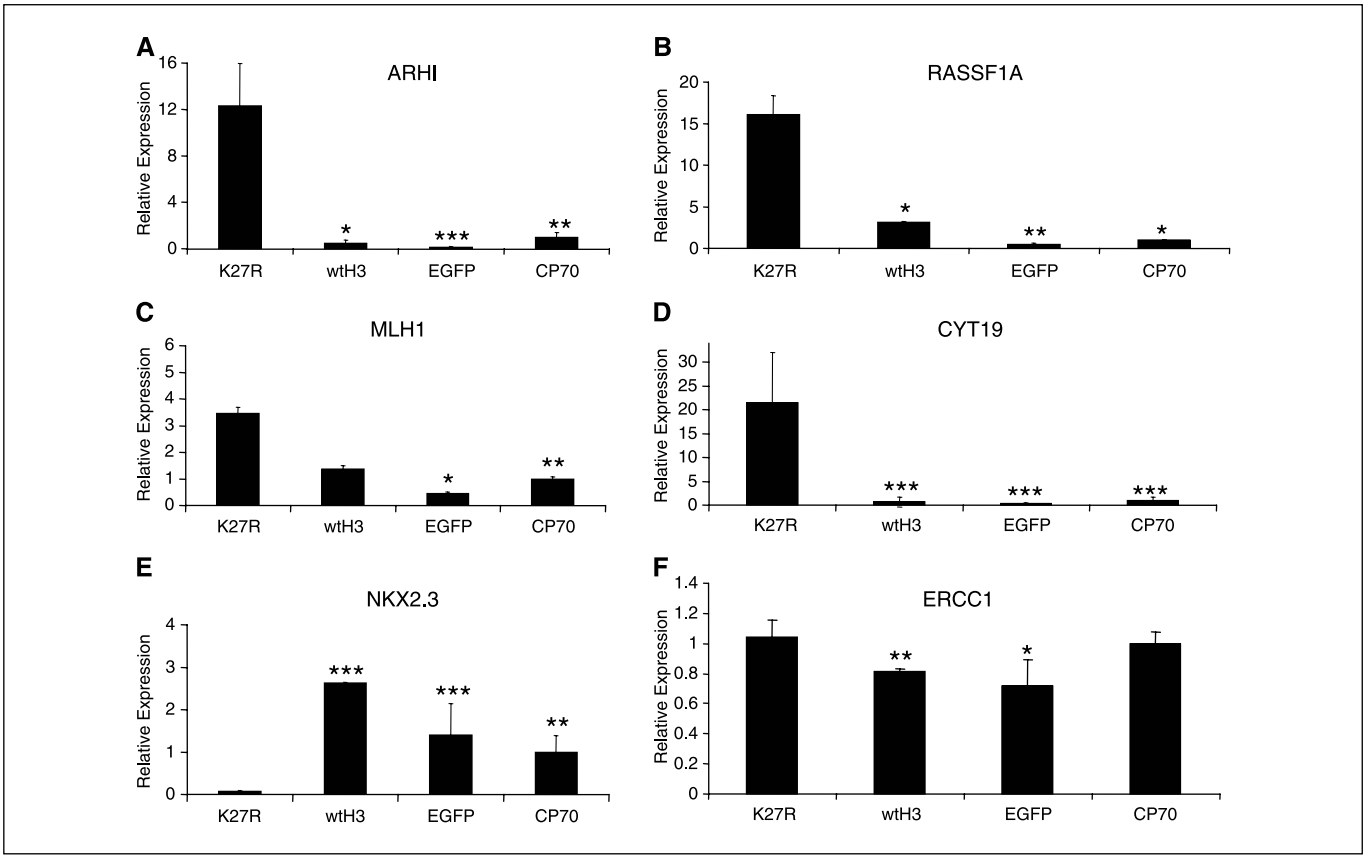

Figure 2. Gene expression analysis in H3-K27R cell versus control cell lines. Target gene expression (*A,* ARHI; *B,* RASSF1A; *C,* hMLH1; *D,* CYT19; *E,* NKX2.3; *F,* ERCC1) was assessed by reverse transcription-quantitative PCR and normalized using *GUSB* or *ACTB* as internal controls. *, $P < 0.05$; **, $P < 0.01$; ***, $P < 0.001$ (*t* test).

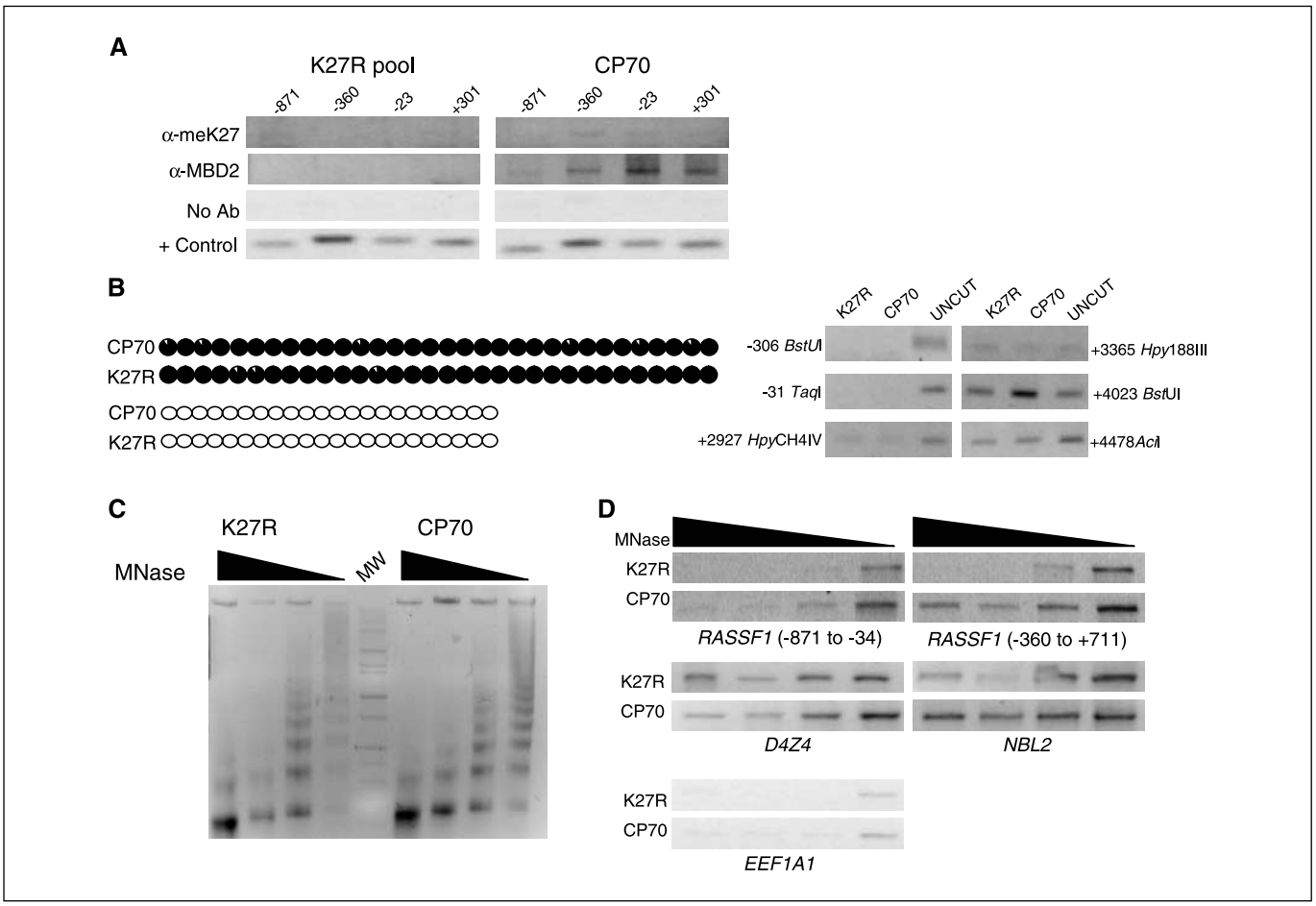

Figure 3. Chromatin environment containing *RASSF1* is altered in K27R cells. *A,* chromatin immunoprecipitation analysis of the *RASSF1* upstream region reveals that H3-$(me)_3$-K27 and MBD2 are present at the *RASSF1* CpG island in CP70 cells but not in H3-K27R pool cells. *B,* bisulfite sequencing (*left*) and COBRA (*right*) analysis of two *RASSF1* CpG islands in K27R cell and control cells. No difference in DNA methylation was seen in the upstream or intronic CpG islands between cell lines. *C,* micrococcal nuclease (*MNase*) digest analysis of H3-K27R and CP70 cells. *MW,* DNA ladder. *D,* PCR analysis of micrococcal nuclease–digested DNA from H3-K27R and CP70 cells using recombined chromatin immunoprecipitation PCR primers. *D4Z4* and *NBL2* are heterochromatic repeats partially hypomethylated in cancer. *EEF1A1* is a highly expressed translation elongation factor.

expression was seen in wtH3 and EGFP cells (Fig. 2*F*). In fact, *ERCC1* was highly expressed in all cell lines (detectable after 21 PCR cycles, compared with 17 cycles for EF1α), indicating that they probably retain the capacity to repair DNA through nucleotide excision repair.

Following assessment of *ERCC1* expression (and indirectly, DNA repair capacity), we directly examined repair of platinum damage. Previous studies have shown that the initial phase of platinum adduct removal from DNA occurs maximally at 6 hours; this removal is directly related to cell survival (34). Therefore, we allowed cell lines to recover for 6 hours after treatment with cisplatin. In one experiment, CP70 and K27R cells were each treated with an IC_{50} dose of cisplatin (10 μmol/L for K27R and 40 μmol/L for CP70). In the second experiment, both cell lines were treated with a 30 μmol/L dose of cisplatin, followed by a 6-hour recovery. Platinum adducts were measured after both experiments. In CP70 cells, 52% of lesions were repaired after the IC_{50} dose, compared with 22% in K27R cells (Fig. 5*B*). Similarly, 44% of the lesions were repaired after 30 μmol/L cisplatin in CP70 cells, compared with just 8% in K27R cells (Fig. 5*C*). Thus, whereas both cell lines probably retain the capacity to repair platinum adducts, CP70 cells are 2- to 5-fold more efficient at adduct repair compared with K27R.

To further investigate whether the H3-meK27 modification was associated with DNA repair, H3-$(me)_3$-K27 levels before and after cisplatin exposure of CP70 cells were examined. Cells were treated with the drug for 3 hours followed by a 3-hour recovery period. After treatment with 40 μmol/L cisplatin, H3-$(me)_3$-K27 levels were increased ($P < 0.01$; Fig. 5*D*), suggesting that the H3-meK27 modification is associated with DNA repair and that loss of H3-K27 methylation may prevent platinum adduct repair. Collectively, the above observations indicate that although altered repair of K27R cells probably does not explain the difference in initial platinum adduct formation, loss of DNA repair seems to lead to persistent adducts, which may in turn enhance antiproliferative or death signals. Because some forms DNA repair, proliferation, and transcription are coupled (35), the loss of H3-K27 methylation could affect all three biological processes by altering only one of the three.

To more directly assess whether DNA-damaging agents interact with DNA in a context-dependent manner (i.e., within euchromatin and not heterochromatin), we used doxorubicin, another DNA-targeting chemotherapeutic agent. Doxorubicin fluoresces, making it possible to localize the drug within cells as described in Materials and Methods. No qualitative chromatin differences between K27R

and CP70 cells were seen with DAPI only (Fig. 6*A* and *B*). Doxorubicin-stained cells showed no signal at the DAPI emission wavelength and DAPI showed no emission at the doxorubicin emission wavelength (not shown). Drug localization within DAPI-poor regions in CP70 nuclei was clearly observed (Fig. 6*C*). We also quantitated the amount of overlapping signals within image planes (n = 17). This analysis showed that 6.4 ± 3.0% of the DAPI signal was overlapped by doxorubicin and 5.7 ± 2.8% of the doxorubicin was overlapped by DAPI. This finding supports the notion that doxorubicin, and probably other DNA-damaging agents like cisplatin, preferentially targets euchromatin. However, no difference

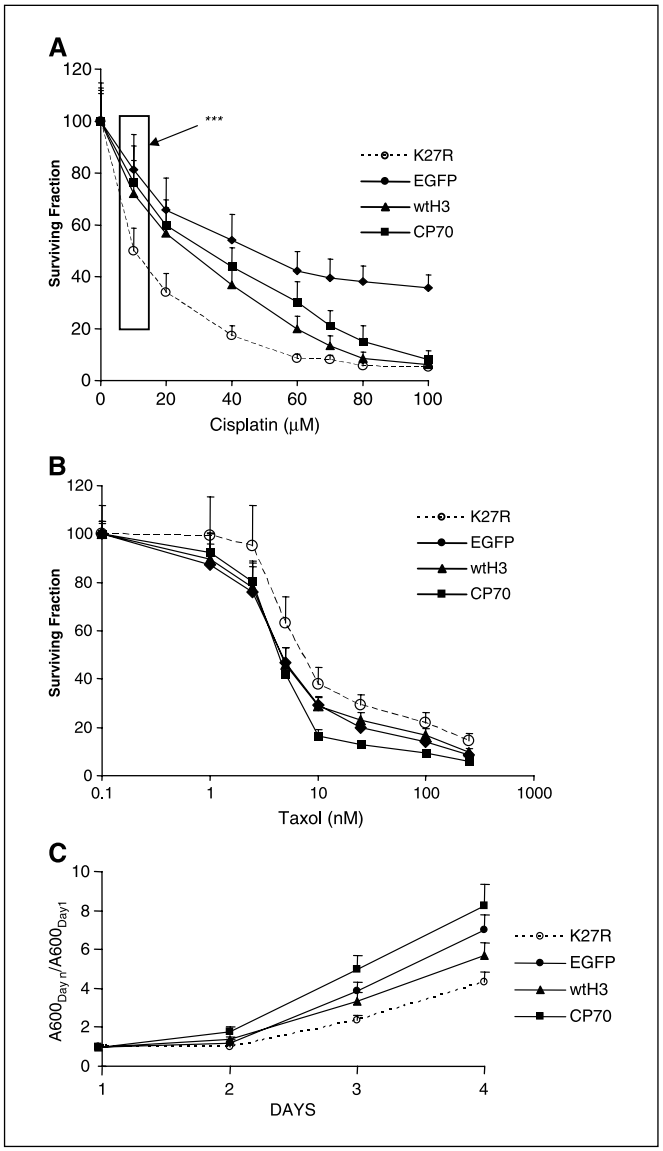

Figure 4. Effect of H3-K27 hypomethylation on chemosensitivity and cell proliferation. *A,* K27R cells are sensitized to cisplatin. Cells were treated for 3 hours with cisplatin followed by a 3-day recovery period. Cell proliferation was assessed using MTT assays (n = 8 experiments) as described in Materials and Methods. The IC_{50} for cisplatin was significantly lower for K27R cells versus CP70 (IC_{50} of 10 versus 40 μmol/L, respectively). *Bars,* SD. ***, $P < 0.001$ (t test). test). *B,* cells were treated with paclitaxel overnight followed by a 2-day recovery period. No difference in IC_{50} for paclitaxel was observed for control and K27R cells. *Bars,* SD. *C,* cell growth rates were determined by measuring MTT absorbance each day for 4 days (n = 16 experiments). Cell growth rates on days 3 and 4 were slightly reduced in K27R cells compared with control cells. *Bars,* SD.

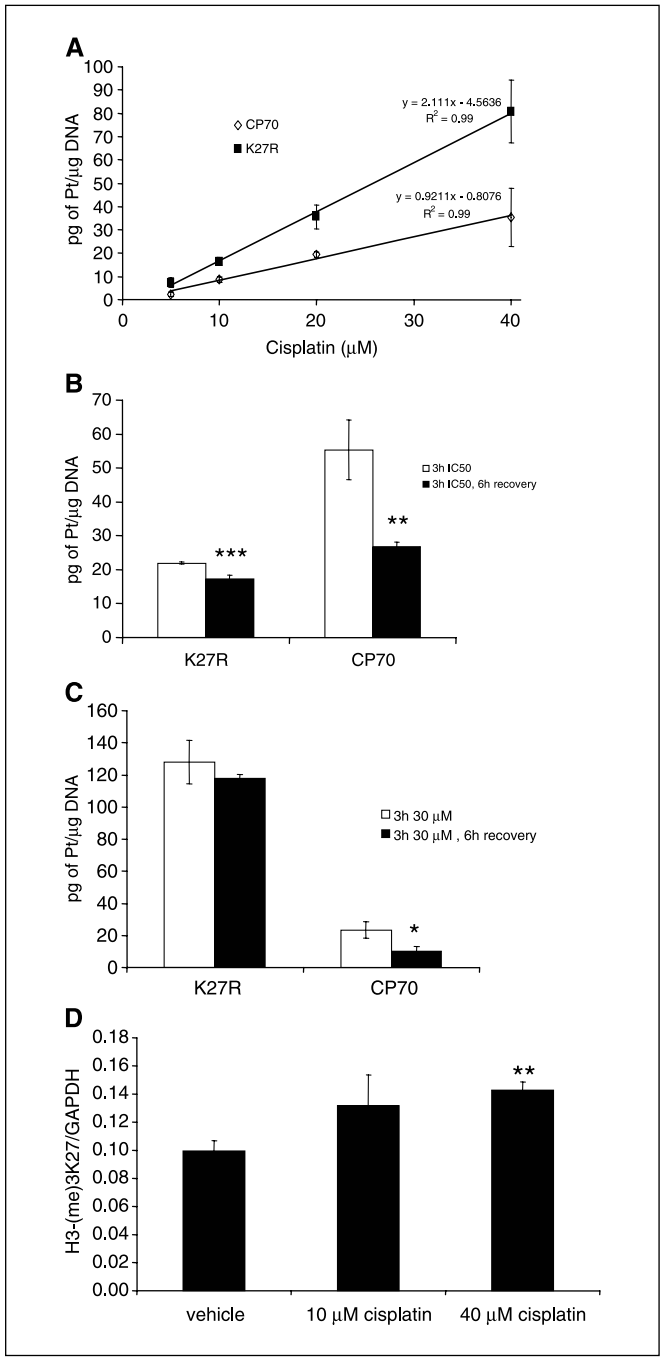

Figure 5. Platinum adducts in DNA after cisplatin treatment of K27R and CP70 cells. *A* to *C,* atomic absorption spectroscopy was used to measure platinum adducts as described in Materials and Methods. *A,* as a function of cisplatin dose, H3-K27R cells acquired twice the DNA damage as CP70 cells ($P < 0.0001$, by SAS). *Points,* average of four samples; *bars,* SD. *B* and *C,* more efficient repair of DNA adducts in CP70 cells versus H3-K27R cells. Cells were treated with an IC_{50} dose of cisplatin (10 and 40 μmol/L for K27R and CP70, respectively) for 3 hours followed by a 6-hour recovery period or no recovery. CP70 cells repaired 52% of adducts compared with only 22% in K27R cells. *Columns,* average of four samples; *bars,* SD. *C,* cells were treated with an 30 μmol/L dose of cisplatin for 3 hours followed by a 6-hour recovery period or no recovery. In CP70 cells, 44% of lesions were repaired compared with only 8% in K27R cells. *Columns,* average of four samples; *bars,* SD. *D,* H3-$(me)_3$-K27 levels were monitored by Western blot analysis before and after treatment with 10 and 40 μmol/L cisplatin. The level of H3-$(me)_3$-K27 tended to increase (33%; $P = 0.08$) after treatment with 10 μmol/L cisplatin; however, a 44% increase ($P < 0.01$) in H3-$(me)_3$-K27 level was observed after treatment with 40 μmol/L cisplatin. *Columns,* average of four samples; *bars,* SE. *, $P < 0.05$; **, $P < 0.01$; ***, $P < 0.001$ (t test unless otherwise specified).

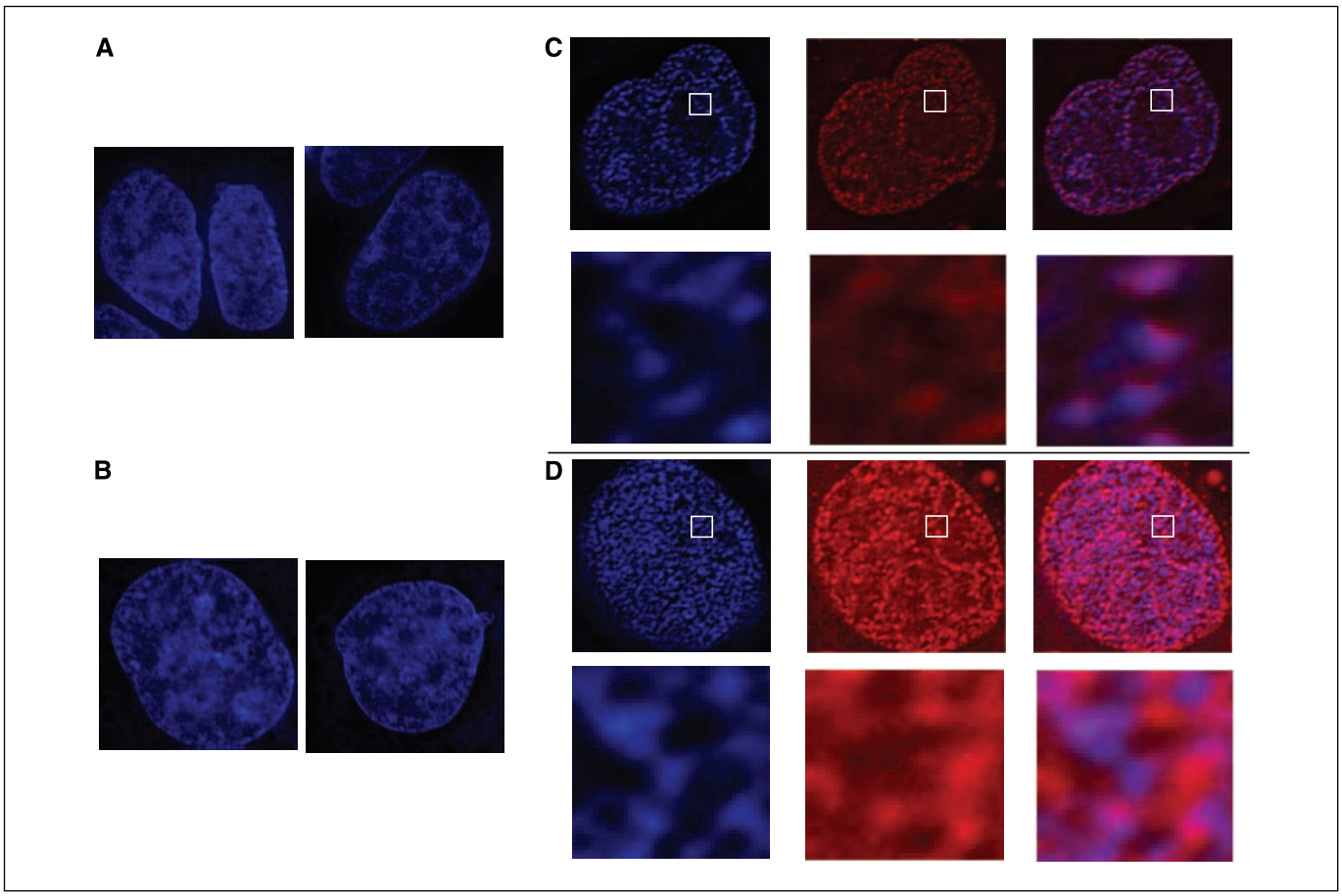

Figure 6. Doxorubicin localizes to DAPI-poor regions within nuclei. K27R (*A*) and CP70 (*B*) cells were stained with DAPI to monitor chromatin conformation. *C* and *D,* CP70 cells were treated with 10 nmol/L doxorubicin for 4 hours, fixed, and stained with DAPI (*blue*) and analyzed for doxorubicin fluorescence localization (*red*). *C* and *D, bottom,* higher magnifications of the nuclear region contained in the white box.

in doxorubicin sensitivity was observed for K27R and CP70 (data not shown), indicating that multiple factors, such as accessibility of the target, differential gene expression, and cellular capacity for DNA repair, determine cellular responses to DNA damaging agents.

Discussion

Histone modifications are clearly implicated in many fundamental aspects of DNA biochemistry, including activation and repression of gene transcription. In the present study, we engineered cancer cells to overexpress high levels of a mutant histone incapable of modification by methylation. By doing so, we established a novel system for investigating specific aspects of the histone code. As previous studies have depended on arduous gene knockouts of multiple, redundant chromatin-modifying enzymes, we offer an alternative approach. While K27R cells still expressed endogenous H3, preventing an absolute knockdown of methylation of that lysine, dramatic effects were nevertheless observed. These included loss of DNA methylation and significant alterations in gene expression patterns, suggesting that our approach is highly relevant to the study of the histone code in cancer cells. Loss of H3-K27 methylation and subsequent resensitization of ovarian cancer cells to cisplatin may have been due to increased tumor suppressor gene expression, increased accessibility to DNA by the drug, and/or a yet undefined role for H3-K27 in DNA adduct repair.

H3-K27 methytransferase activity has been identified as a key component of several repressive Polycomb complexes that mediate gene silencing (2, 3, 7). EZH2, a component of the Polycomb complex, is the primary H3-K27 methyltransferase identified thus far (2, 7, 36). Therefore, many of the K27R cell characteristics we observed could likely be due to reversal of Polycomb target gene silencing by EZH2, although we were not able to confirm this by functional knockdown of EZH2. However, although we observed decreased DNA methylation in K27R cells, DNA methyltransferase activity has yet to be associated with Polycomb complexes or G9a, another H3-K27 methyltransferase. Nonetheless, specific methylated genes have been associated with DNA methylation and Polycomb-mediated silencing (21, 37, 38), supporting our current findings. For example, Mager et al. (39) showed biallelic expression of parentally imprinted loci in PcG gene *Eed* knockout mouse embryos. In that study, although overall DNA methylation at imprinted loci was not reduced, altered DNA methylation patterns of the imprinted loci were observed (39). Further, Fujii et al. (40) reported that increased expression of the maternally imprinted tumor suppressor gene *ARHI* in breast cancer cells was associated with decreased histone H3-K9 methylation. Our finding that ARHI gene expression was increased in K27R cells suggests that H3-K27 methylation may also play a role in *ARHI* gene regulation in ovarian cancer. As cross-talk between histone methylation and DNA methylation has been shown in humans (41–43), mice (19), and

Neurospora crassa (20), an association between DNA methylation and H3-K27 is conceivable.

In addition to altered DNA methylation, we found that loss of H3-K27 methylation resulted in increased platinum sensitivity in chemoresistant cells, which may be due, in part, to changes in expression of genes known to be involved in tumorigenesis, apoptosis, and platinum resistance. For example, the gene encoding the mismatch repair protein hMLH1, strongly established as involved in platinum therapy response in ovarian cancer and frequently methylated in drug-resistant tumors and cell lines (including CP70 cells; ref. 23), was significantly induced in K27R cells. We also found RASSF1A expression to be greatly increased in K27R cells. *RASSF1* is frequently methylated in several types of cancer, including epithelial ovarian (25), although little is known about its function. Whereas *RASSF1* is methylated in CP70 cells, it does not seem to be hypomethylated in K27R cells, although loss of MBD2 occupancy, increased accessibility to nucleases, and increased *RASSF1* transcription would suggest a more permissive chromatin environment. As cisplatin response effects several signal cascades/networks (44), our finding of altered expression of several key components of those networks supports the notion that H3-K27 methylation plays a significant role in platinum resistance.

As cisplatin acts by cross-linking DNA, the formation of DNA-platinum adducts is the result of both drug access to DNA and removal of adducts by the nucleotide excision repair pathway (32). After treatment with cisplatin, we observed a 2- to 4-fold increase in platinum adducts at equivalent doses in K27R cells as compared with CP70 cells. Because platinum adducts were measured immediately after treatment, it is unlikely that a loss or absence of DNA repair played a significant role. The fact that high levels of ERCC1, a critical mediator of the nucleotide excision repair pathway induced by chemotherapy (32), were observed in both cell lines further supports this notion. Thus, the increased platinum adduct formation in K27R cells may be due to a change in the composition or structure of target DNA (i.e., euchromatinization of DNA), a possibility supported by several recent reports showing that chromatin decondensation can enhance DNA-drug interactions (45–47).

Whereas increased platinum adduct formation in K27R cells was not due to disrupted DNA repair capacity (as indicated by ERCC-1 expression), diminished repair was observed following a 6-hour recovery period. We observed a 44% increase in H3-$(me)_3$-K27 in CP70 cells treated with an IC_{50} dose of cisplatin, suggesting that increased cisplatin sensitivity in K27R cells may be due to loss of capacity to methylate H3-K27. These observations are suggestive of a more direct role for histone methylation in DNA repair, perhaps by recruiting chromatin-binding proteins to sites of damage and/or by regulating DNA checkpoint responses (48–50).

It has been previously shown that the activity of multiple DNA repair pathways, including that of the nucleotide excision repair pathway, is enhanced at sites of transcription (35). Based on the loss of heterochromatic structures and the associated up-regulation of gene expression in K27R cells, we speculated that in K27R cells, DNA repair would be more efficient. Somewhat surprisingly, however, the ability of K27R cells to repair cisplatin damage was impaired; furthermore, K27R cells contained more sites of DNA damage after treatment with cisplatin (versus CP70 cells). Based on these observations, we postulate that many of the lesions occurred at sites of transcription. Increased cell death signaling by damage-sensing machinery at sites of adduction may preclude repair, resulting in increased chemosensitivity in K27R cells.

In summary, we have shown that H3-meK27 methylation and DNA methylation are interrelated chromatin modifications and present the first evidence for H3-K27 methylation in cancer chemotherapy resistance. The mechanism of resistance reversal on loss of H3-K27 methylation is likely due to altered gene expression, as well as global changes in chromatin structure that result in increased susceptibility to damage by a DNA-targeting agent. Model systems such as ours may allow for further insight into the role of histone code modifications in tumor progression and the acquisition of chemoresistance.

Acknowledgments

Received 10/5/2005; revised 2/12/2006; accepted 3/28/2006.

Grant support: NIH grants CA8529 (K.P. Nephew) and U54CA11300 (T.H.M. Huang).

The costs of publication of this article were defrayed in part by the payment of page charges. This article must therefore be hereby marked *advertisement* in accordance with 18 U.S.C. Section 1734 solely to indicate this fact.

We thank Professors Robert Brown (Beatson Cancer Center, University of Glasgow), Thomas Jenuwein (University of Vienna), and Paul Wade (National Institute of Environmental Health Sciences) for providing valuable reagents used in this study, and Barry Stein, Min Choi, and Teresa Craft for excellent technical support.

References

1. Lewis EB. A gene complex controlling segmentation in *Drosophila*. Nature 1978;276:565–70.
2. Cao R, Wang L, Wang H, et al. Role of histone H3 lysine 27 methylation in Polycomb-group silencing. Science 2002;298:1039–43.
3. Otte AP, Kwaks TH. Gene repression by Polycomb group protein complexes: a distinct complex for every occasion? Curr Opin Genet Dev 2003;13:448–54.
4. Kuzmichev A, Margueron R, Vaquero A, et al. Composition and histone substrates of polycomb repressive group complexes change during cellular differentiation. Proc Natl Acad Sci U S A 2005;102:1859–64.
5. Cao R, Zhang Y. The functions of E(Z)/EZH2-mediated methylation of lysine 27 in histone H3. Curr Opin Genet Dev 2004;14:155–64.
6. Kirmizis A, Bartley SM, Kuzmichev A, et al. Silencing of human polycomb target genes is associated with methylation of histone H3 Lys 27. Genes Dev 2004;18:1592–605.
7. Muller J, Hart CM, Francis NJ, et al. Histone methyltransferase activity of a *Drosophila* Polycomb group repressor complex. Cell 2002;111:197–208.
8. Varambally S, Dhanasekaran SM, Zhou M, et al. The polycomb group protein EZH2 is involved in progression of prostate cancer. Nature 2002;419:624–9.
9. Kleer CG, Cao Q, Varambally S, et al. EZH2 is a marker of aggressive breast cancer and promotes neoplastic transformation of breast epithelial cells. Proc Natl Acad Sci U S A 2003;100:11606–11.
10. Kirmizis A, Bartley SM, Farnham PJ. Identification of the polycomb group protein SU(Z)12 as a potential molecular target for human cancer therapy. Mol Cancer Ther 2003;2:113–21.
11. Jenuwein T, Allis CD. Translating the histone code. Science 2001;293:1074–80.
12. Strahl BD, Allis CD. The language of covalent histone modifications. Nature 2000;403:41–5.
13. Peters AH, O'Carroll D, Scherthan H, et al. Loss of the Suv39h histone methyltransferases impairs mammalian heterochromatin and genome stability. Cell 2001;107:323–37.
14. Tachibana M, Sugimoto K, Nozaki M, et al. G9a histone methyltransferase plays a dominant role in euchromatic histone H3 lysine 9 methylation and is essential for early embryogenesis. Genes Dev 2002;16:1779–91.
15. Behrens BC, Hamilton TC, Masuda H, et al. Characterization of a *cis*-diamminedichloroplatinum(II)-resistant human ovarian cancer cell line and its use in evaluation of platinum analogues. Cancer Res 1987;47:414–8.
16. Levenstein ME, Kadonaga JT. Biochemical analysis of chromatin containing recombinant *Drosophila* core histones. J Biol Chem 2002;277:8749–54.
17. Stach D, Schmitz OJ, Stilgenbauer S, et al. Capillary electrophoretic analysis of genomic DNA methylation levels. Nucleic Acids Res 2003;31:E2.
18. Cha TL, Zhou BP, Xia W, et al. Akt-mediated phosphorylation of EZH2 suppresses methylation of lysine 27 in histone H3. Science 2005;310:306–10.
19. Lehnertz B, Ueda Y, Derijck AA, et al. Suv39h-mediated histone H3 lysine 9 methylation directs DNA methylation to major satellite repeats at pericentric heterochromatin. Curr Biol 2003;13:1192–200.
20. Tamaru H, Selker EU. A histone H3 methyltransferase controls DNA methylation in *Neurospora crassa*. Nature 2001;414:277–83.

21. Xin Z, Tachibana M, Guggiari M, et al. Role of histone methyltransferase G9a in CpG methylation of the Prader-Willi syndrome imprinting center. J Biol Chem 2003;278:14996–5000.

22. Yang AS, Estecio MR, Doshi K, et al. A simple method for estimating global DNA methylation using bisulfite PCR of repetitive DNA elements. Nucleic Acids Res 2004; 32:e38.

23. Strathdee G, MacKean MJ, Illand M, et al. A role for methylation of the hMLH1 promoter in loss of hMLH1 expression and drug resistance in ovarian cancer. Oncogene 1999;18:2335–41.

24. Yu Y, Xu F, Peng H, et al. NOEY2 (ARHI), an imprinted putative tumor suppressor gene in ovarian and breast carcinomas. Proc Natl Acad Sci U S A 1999;96:214–9.

25. Ibanez de Caceres I, Battagli C, Esteller M, et al. Tumor cell-specific BRCA1 and RASSF1A hypermethylation in serum, plasma, and peritoneal fluid from ovarian cancer patients. Cancer Res 2004;64:6476–81.

26. Whiteside MA, Chen DT, Desmond RA, et al. A novel time-course cDNA microarray analysis method identifies genes associated with the development of cisplatin resistance. Oncogene 2004;23:744–52.

27. Fraga MF, Ballestar E, Villar-Garea A, et al. Loss of acetylation at Lys16 and trimethylation at Lys20 of histone H4 is a common hallmark of human cancer. Nat Genet 2005;37:391–400.

28. Balch C, Yan P, Craft T, et al. Antimitogenic and chemosensitizing effects of the methylation inhibitor zebularine in ovarian cancer. Mol Cancer Ther 2005;4: 1505–14.

29. Plumb JA, Strathdee G, Sludden J, et al. Reversal of drug resistance in human tumor xenografts by 2′-deoxy-5-azacytidine-induced demethylation of the hMLH1 gene promoter. Cancer Res 2000;60:6039–44.

30. Peters AH, Kubicek S, Mechtler K, et al. Partitioning and plasticity of repressive histone methylation states in mammalian chromatin. Mol Cell 2003;12:1577–89.

31. Fishel ML, Delaney SM, Friesen LD, et al. Enhancement of platinum-induced cytotoxicity by O^6-benzylguanine. Mol Cancer Ther 2003;2:633–40.

32. Reed E. Platinum-DNA adduct, nucleotide excision repair and platinum based anti-cancer chemotherapy. Cancer Treat Rev 1998;24:331–44.

33. Westerveld A, Hoeijmakers JH, van Duin M, et al. Molecular cloning of a human DNA repair gene. Nature 1984;310:425–9.

34. Parker RJ, Eastman A, Bostick-Bruton F, et al. Acquired cisplatin resistance in human ovarian cancer cells is associated with enhanced repair of cisplatin-DNA lesions and reduced drug accumulation. J Clin Invest 1991;87:772–7.

35. Friedberg EC, Walker GC, Siede W. DNA repair and mutagenesis. Washington (DC): ASM Press; 1995.

36. Tachibana M, Sugimoto K, Fukushima T, et al. Set domain-containing protein, G9a, is a novel lysine-preferring mammalian histone methyltransferase with hyperactivity and specific selectivity to lysines 9 and 27 of histone H3. J Biol Chem 2001;276:25309–17.

37. Chen H, Tu SW, Hsieh JT. Down-regulation of human DAB2IP gene expression mediated by polycomb Ezh2 complex and histone deacetylase in prostate cancer. J Biol Chem 2005;280:22437–44.

38. Leu YW, Yan PS, Fan M, et al. Loss of estrogen receptor signaling triggers epigenetic silencing of downstream targets in breast cancer. Cancer Res 2004; 64:8184–92.

39. Mager J, Montgomery ND, de Villena FP, et al. Genome imprinting regulated by the mouse Polycomb group protein Eed. Nat Genet 2003;33:502–7.

40. Fujii S, Luo RZ, Yuan J, et al. Reactivation of the silenced and imprinted alleles of ARHI is associated with increased histone H3 acetylation and decreased histone H3 lysine 9 methylation. Hum Mol Genet 2003; 12:1791–800.

41. Nguyen CT, Weisenberger DJ, Velicescu M, et al. Histone H3-lysine 9 methylation is associated with aberrant gene silencing in cancer cells and is rapidly reversed by 5-aza-2′-deoxycytidine. Cancer Res 2002;62:6456–61.

42. Bachman KE, Park BH, Rhee I, et al. Histone modifications and silencing prior to DNA methylation of a tumor suppressor gene. Cancer Cell 2003;3:89–95.

43. Espada J, Ballestar E, Fraga MF, et al. Human DNA methyltransferase 1 is required for maintenance of the histone H3 modification pattern. J Biol Chem 2004;279: 37175–84.

44. Siddik ZH. Cisplatin: mode of cytotoxic action and molecular basis of resistance. Oncogene 2003;22:7265–79.

45. Kim MS, Blake M, Baek JH, et al. Inhibition of histone deacetylase increases cytotoxicity to anticancer drugs targeting DNA. Cancer Res 2003;63:7291–300.

46. Marchion DC, Bicaku E, Daud AI, et al. Sequence-specific potentiation of topoisomerase II inhibitors by the histone deacetylase inhibitor suberoylanilide hydroxamic acid. J Cell Biochem 2004;92:223–37.

47. Marchion DC, Bicaku E, Daud AI, et al. Valproic acid alters chromatin structure by regulation of chromatin modulation proteins. Cancer Res 2005;65:3815–22.

48. Giannattasio M, Lazzaro F, Plevani P, et al. The DNA damage checkpoint response requires histone H2B ubiquitination by Rad6-Bre1 and H3 methylation by Dot1. J Biol Chem 2005;280:9879–86.

49. Huyen Y, Zgheib O, Ditullio RA, Jr., et al. Methylated lysine 79 of histone H3 targets 53BP1 to DNA double-strand breaks. Nature 2004;432:406–11.

50. Sanders SL, Portoso M, Mata J, et al. Methylation of histone H4 lysine 20 controls recruitment of Crb2 to sites of DNA damage. Cell 2004;119:603–14.